Pinning down HER2–ER crosstalk in SMRT regulation

Akihide Ryo[1], Gerburg Wulf[2], Tae Ho Lee[2] and Kun Ping Lu[2]

[1] AIDS Research Center, National Institute of Infectious Diseases, 1-23-1 Toyama, Shinjuku-ku, Tokyo 162-8640, Japan

[2] Department of Medicine, Beth Israel Deaconess Medical Center, Harvard Medical School, 330 Brookline Avenue, CLS0408, Boston, MA 02215, USA

Corresponding authors: Lu, K. P. (klu@bidmc.harvard.edu); Ryo, A. (aryo@nih.go.jp).

SMRT (silencing mediator for retinoic acid and thyroid hormone receptors) is a transcriptional co-repressor that mediates the repressive function of nuclear hormone receptors such as the estrogen receptor (ER). Decreased SMRT levels correlate with acquired tamoxifen resistance in breast cancer, and SMRT restoration might resensitize breast cancer cells to tamoxifen. A new study demonstrates that SMRT protein stability is regulated by phosphorylation-dependent Pin1-catalyzed prolyl-isomerization. Pin1 functions downstream of HER2, positioning it as an important modulator of the crosstalk between ER and growth factor signaling.

Breast cancer and the estrogen receptor

Breast cancer is one of the most common malignancies in women and the second most common cause of female cancer-related deaths [1]. However, deaths due to breast cancer have decreased in recent years owing to the development of targeted therapies, including hormone therapy, in addition to conventional chemotherapy and surgical interventions [1]. The majority of breast cancers in post-menopausal women express the estrogen receptor (ER), and after surgery they can be treated with hormonal therapy alone, in the absence of more toxic chemotherapy, resulting in a relatively favorable prognosis [2]. However, a significant fraction of these hormone-sensitive breast cancer patients will experience disease progression that is attributable to the resistance to endocrine agents, such as tamoxifen, thus resulting in mortality [3]. Therefore, it is desirable to develop new strategies to treat hormone refractory breast cancer; this goal will probably be facilitated by elucidating the underlying molecular mechanisms of hormone resistance. A new study by Stanya and colleagues [4] delineates an important hint in solving the riddle of endocrine resistance. They find that Cdk2 (cyclin dependent kinase 2)-mediated phosphorylation of SMRT (silencing mediator for retinoid and thyroid receptors), an ER co-repressor, creates binding sites for protein (peptidyl-prolyl cis/trans isomerase) NIMA-interacting 1 (Pin1), which in turn induces conformational changes to promote SMRT degradation (Figure 1a). Moreover, this event crucially mediates human epidermal growth factor receptor 2 (HER2)-dependent SMRT protein degradation and resultant endocrine resistance. These findings shed new light on the molecular mechanism of SMRT regulation and warrant further investigation of the role and therapeutic potential of Pin1 in the treatment of endocrine-resistant breast cancers.

ER regulation

ER is a member of the nuclear hormone receptor family, which has important roles in cell proliferation, differentiation and oncogenesis [5]. In response to the hormone estrogen, ER can recruit steroid receptor coactivator-3 (SRC-3; also called amplified in breast cancer-1, AIB1) to enhance estrogen-dependent transcriptional gene activation. In the absence of 17β-estradiol (E2), ER can interact with co-repressors such as SMRT and N-CoR (nuclear receptor co-repressor) to repress target gene expression [6]. Although both SMRT and N-CoR mediate the most repressive function of unliganded ER by recruiting histone deacetylase 3 (HDAC3), only SMRT inhibition is sufficient to de-sensitize cells to tamoxifen-mediated inhibition of ER-induced gene expression [7].

Crosstalk between HER2 and ER

HER2 (also known as ErbB2, ERBB2 and Neu) is a member of the epidermal growth factor receptor family that has a notable role in breast cancer pathogenesis; it is the target of the anti-breast-cancer drug trastuzumab [8]. Both preclinical and clinical evidence implicates HER2 overexpression in the development of endocrine resistance, especially to tamoxifen [9]. The receptor crosstalk between the ER and growth factor receptors affects ER transcriptional activity. For example, HER2-dependent mitogen-activated protein kinase (MAPK) activation triggers both ER and SRC-3 phosphorylation thereby increasing their transcriptional activity [10,11]. MAPK can also phosphorylate SMRT thereby reducing its binding affinity for transcription factors and enhancing its nuclear export [12]. However, it is unknown whether growth factor signaling modulates

co-repressor stability. Several previous reports indicate that estrogen markedly downregulates N-CoR protein levels in ER-positive breast cancer cells without affecting SMRT levels [13]. Therefore, it will be of great importance to elucidate the regulatory mechanism(s) underlying SMRT stability in relation to tamoxifen resistance and growth-factor signaling in breast cancer.

The role of Pin1 in HER2–ER crosstalk

The peptidyl-prolyl isomerase Pin1 is an important regulator in HER2-mediated growth signaling and ER-mediated transcription in breast cancer [14]. Unlike other prolyl isomerases, Pin1 binds to discrete phosphorylated Ser/Thr-Pro motifs in a specific group of proteins and catalyzes their *cis–trans* isomerization to regulate protein conformation as a mode of post-phosphorylation regulation. Such Pin1-catalyzed prolyl isomerization can regulate a wide spectrum of phosphorylation-dependent activities, including protein stability [14]. Importantly, Pin1 is highly overexpressed in several human cancers including breast cancer, and its expression levels parallel the malignant properties of many tumors [14,15]. Pin1 is transcriptionally upregulated by the E2F transcription factors in response to growth factors and other stimulating conditions such as HER2 or Ras activation in breast cancer [16]. Moreover, Pin1 inhibition or deletion efficiently suppresses the ability of oncogenic HER2 or Ras to transform normal mammary epithelial cells or to induce breast cancer *in vivo* [16,17]. Thus, Pin1 is essential for growth-factor-induced breast cancer development.

A previous report indicated that Pin1 can regulate SRC-3 activity and turnover [18]. Pin1 binds to phosphorylated SRC-3 and enhances SRC-3-mediated recruitment of cAMP-response-element binding protein (CREB) binding protein (CBP; similar to p300) to the promoters of ER-dependent genes to activate transcription. In addition, Pin1 enhances SRC-3 degradation, an event that seems to promote SRC-3 turnover and sustained activation, rather than its functional attenuation, although a detailed mechanism remains elusive [18]. It remains unclear whether Pin1 can regulate transcriptional co-repressors during and after oncogenesis or whether Pin1 participates in hormone therapy resistance in conjunction with aberrant growth-factor signaling in breast cancers.

Newly identified: Pin1-dependent SMRT regulation

Stanya and colleagues [4] now provide the first evidence that Pin1-catalyzed, phosphorylation-dependent prolyl isomerization promotes SMRT protein degradation, thereby reducing SMRT-mediated ER transcriptional repression. The authors first identified Pin1 as a SMRT interacting partner in a yeast two-hybrid screen, and they confirmed that this interaction relies upon the Pin1 Trp-Trp domain binding phosphorylated SMRT.

One of the functional consequences of the Pin1–SMRT association is to promote SMRT degradation. As Pin1 overexpression compromises SMRT repressor activity, Stanya and colleagues [4] hypothesized that Pin1 might modulate SMRT-mediated repression by affecting its protein stability, as has been shown for other Pin1 targets [14,19]. Indeed, Pin1 overexpression promoted SMRT protein degradation in a dose-dependent manner, whereas Pin1 knockdown or knockout significantly increased SMRT stability. Moreover, the effects of Pin1 knockdown on SMRT stability could be rescued by ectopic Pin1 expression, but not expression of its catalytically inactive mutant [4]. The authors thus concluded that Pin1 regulates SMRT protein half-life.

The authors then mapped the Pin1-binding sites in SMRT via mutational analysis. They also identified multiple Ser and Thr residues in SMRT that are phosphorylated *in vivo*, including two consensus Cdk target sites: Ser1241 and Ser1469. Indeed, Pin1 can interact with SMRT on these two sites *in vitro*. Furthermore, a triple mutant at 3 potential Cdk consensus sites (Ser1241Ala; Thr1445Ala; Ser1469Ala) is neither phosphorylated by Cdk2 nor pulled down by Pin1. Importantly, the SMRT triple mutant is also more stable than wild-type SMRT. In addition, Cdk2 overexpression can reduce exogenous SMRT protein levels, which can be rescued by Pin1 knockdown [4]. Furthermore, siRNA-mediated Cdk2 knockdown upregulates endogenous SMRT levels. These data indicate that SMRT phosphorylation by Cdk2 is crucial for Pin1-mediated SMRT degradation.

HER2 signaling can increase Cdk activity and upregulate Pin1 expression in breast cancers [19,20]. Therefore, Stanya and colleagues [4] next explored how ER activity might be regulated by functional crosstalk between HER2 signaling and the Cdk2- and Pin1-dependent SMRT-degradation pathway. A HER2 agonist, for example heregulin, decreases SMRT protein levels, whereas a HER2 inhibitor, for example AG825, increases both SMRT half-life and protein levels. Moreover, Pin1 or Cdk2 knockdown blocks heregulin from decreasing SMRT stability [4]. These data point to HER2 functioning upstream of Cdk2 and Pin1 as a potential regulator of SMRT protein stability.

Finally, to delineate the possible role of the SMRT degradation pathway in tamoxifen resistance (Box 1), the authors investigated the effect of SMRT, Pin1 or Cdk2 knockdown on ER

activity after tamoxifen treatment of ER-positive breast cancer cells. They found that tamoxifen treatment represses the expression of two different ER target genes; this effect is compromised by SMRT knockdown. By contrast, Pin1 or Cdk2 knockdown enhances the repression of both ER target genes. Moreover, SMRT knockdown increases cell proliferation, whereas Cdk2 inhibition produces a slight decrease in cell proliferation. Interestingly, Pin1 inhibition does not significantly reduce cell growth despite suppressing ER activity. It thus seems that complex crosstalk between Pin1 or Cdk2 and other proteins involved in cell growth might explain the discrepancy between ER-mediated transcription and cell proliferation on increased SMRT stability.

This new study [4] highlights the potential role for Pin1 as a target for preventing improper ER activation; moreover, it could provide important insight toward understanding the nature of tamoxifen resistance in breast cancer. What remains unclear, however, is the mechanism underlying Pin1-dependent SMRT degradation. The identification of factors involved in the Pin1-mediated SMRT-degradation pathway might uncover vital information regarding the enigmatic cell-type-specific function of Pin1 in SMRT regulation. Furthermore, relevant factors could be potential new therapeutic targets for treating hormone-resistant breast cancers. Because Pin1 can bind to many cellular proteins, it becomes important to ask whether Pin1 fosters ER-mediated transcription and hormone resistance only by decreasing SMRT stability. Indeed, because Pin1 can also increase ER function by acting on SRC-3, it could act together with HER2 signaling as a molecular determinant of the balance between ER co-repression and coactivation (Figure 1b). However, it remains unclear why Pin1-mediated degradation of both the coactivator and co-repressor triggers similar ER activation and how these events are coordinated. Further careful analysis of the interplay between Pin1 and relevant signaling pathways will be necessary to fully delineate the function of Pin1 and its target proteins in the regulation of ER and endocrine resistance in breast cancer.

Concluding remarks

Pin1 regulates both the co-repressor SMRT and the coactivator SRC-3 as a downstream effector of HER2 signaling [4,14,16–18]. Growth-factor-receptor signaling is often increased in endocrine-resistant breast tumors, and it contributes to coactivator upregulation and co-repressor downregulation, thus activating proliferation and/or survival pathways and hormone resistance [9,10]. Interestingly, Pin1 inhibitors (if identified) potentially could be administered to re-sensitize tumors to endocrine therapies. Furthermore, such Pin1 inhibitors could be used along with hormonal therapies to block ER proliferation and/or survival activity and the agonistic effects of selective estrogen receptor modulators such as tamoxifen, which both are often deregulated by aberrant growth factor receptor signaling.

Acknowledgements

Work done in our laboratories is supported by National Institutes of Health grants GM58556, AG17870, AG22082 to K.P.L (www.nih.gov).

References

1 Berry, D.A. *et al.* (2005) Effect of screening and adjuvant therapy on mortality from breast cancer. *N. Engl. J. Med.* 353, 1784–1792

2 Joslyn, S.A. (2002) Hormone receptors in breast cancer: racial differences in distribution and survival. *Breast Cancer Res. Treat.* 73, 45–59

3 Dawood, S. and Cristofanilli, M. (2007) Endocrine resistance in breast cancer: what really matters? *Ann. Oncol.* 18, 1289–1291

4 Stanya, K.J. *et al.* (2008) Cdk2 and Pin1 negatively regulate the transcriptional corepressor SMRT. *J. Cell Biol.* 183, 49–61

5 Parker, M.G. (1993) Steroid and related receptors. *Curr. Opin. Cell Biol.* 5, 499–504

6 Xu, L. *et al.* (1999) Coactivator and corepressor complexes in nuclear receptor function. *Curr. Opin. Genet. Dev.* 9, 140–147

7 Privalsky, M.L. (2004) The role of corepressors in transcriptional regulation by nuclear hormone receptors. *Annu. Rev. Physiol.* 66, 315–360

8 Moasser, M.M. (2007) The oncogene HER2: its signaling and transforming functions and its role in human cancer pathogenesis. *Oncogene* 26, 6469–6487

9 Shou, J. *et al.* (2004) Mechanisms of tamoxifen resistance: increased estrogen receptor-HER2/neu cross-talk in ER/HER2-positive breast cancer. *J. Natl. Cancer Inst.* 96, 926–935

10 Osborne, C.K. *et al.* (2005) Crosstalk between estrogen receptor and growth factor receptor pathways as a cause for endocrine therapy resistance in breast cancer. *Clin. Cancer Res.* 11, 865s–870s

11 Font de Mora, J. and Brown, M. (2000) AIB1 is a conduit for kinase-mediated growth factor signaling to the estrogen receptor. *Mol. Cell. Biol.* 20, 5041–5047

12 Jonas, B.A. and Privalsky, M.L. (2004) SMRT and N-CoR corepressors are regulated by distinct kinase signaling pathways. *J. Biol. Chem.* 279, 54676–54686

13 Frasor, J. *et al.* (2005) Estrogen down-regulation of the corepressor N-CoR: mechanism and implications for estrogen derepression of N-CoR-regulated genes. *Proc. Natl. Acad. Sci. U. S. A.* 102, 13153–13157

14 Lu, K.P. and Zhou, X.Z. (2007) The prolyl isomerase Pin1: a pivotal new twist in phosphorylation signalling and human disease. *Nat. Rev. Mol. Cell Biol.* 8, 904–916

15 Wulf, G.M. *et al.* (2001) Pin1 is overexpressed in breast cancer and potentiates the transcriptional activity of phosphorylated c-Jun towards the cyclin D1 gene. *EMBO J.* 20, 3459–3472

16 Ryo, A. *et al.* (2002) Pin1 is an E2F target gene essential for the Neu/Ras-induced transformation of mammary epithelial cells. *Mol. Cell. Biol.* 22, 5281–5295

17 Wulf, G. *et al.* (2004) Modeling breast cancer *in vivo* and *ex vivo* reveals an essential role of Pin1 in tumorigenesis. *EMBO J.* 23, 3397–3407

18 Yi, P. *et al.* (2005) Peptidyl-prolyl isomerase 1 (Pin1) serves as a coactivator of steroid receptor by regulating the activity of phosphorylated steroid receptor coactivator 3 (SRC-3/AIB1). *Mol. Cell. Biol.* 25, 9687–9699

19 Ryo, A. *et al.* (2001) Pin1 regulates turnover and subcellular localization of β-catenin by inhibiting its interaction with APC. *Nat. Cell Biol.* 3, 793–801

20 Neve, R.M. *et al.* (2000) Effects of oncogenic ErbB2 on G1 cell cycle regulators in breast tumour cells. *Oncogene* 19, 1647–1656

21 Riggs, B.L. and Hartmann, L.C. (2003) Selective estrogen-receptor modulators – mechanisms of action and application to clinical practice. *N. Engl. J. Med.* 348, 618–629

22 Fujita, T. *et al.* (2003) Full activation of estrogen receptor α activation function-1 induces proliferation of breast cancer cells. *J. Biol. Chem.* 278, 26704–26714

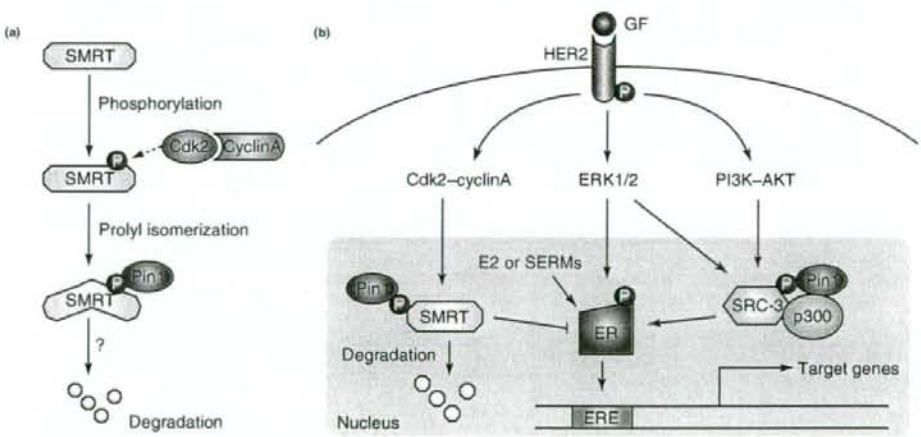

TiBS

Figure 1. Pin1 functions as a crucial catalyst in the crosstalk between HER2 and ER. **(a)** A novel post-phosphorylation regulatory mechanism for SMRT stability. The phosphorylation of SMRT by the proline-directed kinase Cdk2 (shown with its binding partner, cyclinA) generates binding modules for the prolyl isomerase Pin1. Subsequent prolyl isomerization by Pin1 induces conformational changes and thereby enhances SMRT degradation. **(b)** Pin orchestrates signaling cascades from HER2 to ER. Growth-factor-mediated signaling via HER2 activates several downstream kinases, including MAPK (ERK1/2), phosphoinositide 3-kinase (PI3K)–Akt and Cdk2–cyclinA. These kinases, in turn, phosphorylate both the co-repressor SMRT and coactivator SRC-3 (shown in a complex with p300), in addition to ER, creating Pin1-binding sites. Subsequent Pin1-mediated prolyl isomerization activates ER and renders it resistant to SERMs (selective estrogen receptor modulators). These data indicate that Pin1 has a central role in the crosstalk between growth factor signaling and ER during ER-mediated transcription and tamoxifen resistance. GF, growth factor; ERE, estrogen response element.

Box 1. Tamoxifen resistance in breast cancer

Tamoxifen is currently the most widely prescribed orally active selective ER modulator for the treatment of breast cancer [21]. Although tamoxifen is an ER antagonist in breast tissue, it has variable cell-type-specific partial agonist or antagonist activities. The antagonist activity enables the drug to block ER-mediated transcription and cancer cell growth in ER-positive breast cancer cells. However, tamoxifen resistance might occur when its agonistic activity overcomes its antagonistic effect [21]. This variability could be related, in part, to the cellular milieu of ER coactivators and co-repressors [10]. For example, increased levels of coactivators, such as SRC-3, enhance the estrogen agonist properties of tamoxifen, whereas decreased levels of co-repressors, such as SMRT and N-CoR, correlate with acquired tamoxifen resistance [9,10]. Therefore, tamoxifen resistance might depend on the relative abundance or activity between co-repressors and coactivators that are often determined by HER2-iniated upstream growth-factor signaling [22].

FEBS Letters 582 (2008) 2737–2744

DNA-binding profiling of human hormone nuclear receptors via fluorescence correlation spectroscopy in a cell-free system

Tamiyo Kobayashi[a,b], Yoshiko Kodani[a], Akira Nozawa[a,c], Yaeta Endo[a,c,*], Tatsuya Sawasaki[a,c,*]

[a] *Cell-Free Science and Technology Research Center, and The Venture Business Laboratory, Ehime University, 3 Bunkyo-cho, Matsuyama, Ehime 790-8577, Japan*
[b] *Life Science Group, Olympus Corp., 2-3 Kuboyama-cho, Hachioji, Tokyo 192-8512, Japan*
[c] *RIKEN Genomic Sciences Center, 1-7-22 Suehiro-cho, Tsurumi, Yokohama 230-0045, Japan*

Received 11 April 2008; revised 1 July 2008; accepted 1 July 2008

Available online 11 July 2008

Edited by Paul Bertone

Abstract The nuclear hormone receptors (NHRs), a family of transcription factors, bind directly to the hormone response elements (HREs) to regulate gene expression. In this study, we describe a comprehensive NHR–HRE profiling analysis with a new high-throughput DNA binding assay system utilizing wheat germ cell-free protein production and fluorescence correlation spectroscopy (FCS). This approach revealed NHR binding to natural response elements and new heterodimeric NHR–HRE bindings. We analyzed 408 possible binding combinations between 34 human NHRs and 12 different HREs, and identified 205 NHR–HRE binding combinations, 124 of which have not been previously reported. Thus, this study provides a novel biochemical classification of the human NHRs, as well as describing a novel approach to the large-scale analysis of DNA–protein interactions.

Keywords: Cell-free protein production; DNA-binding profiling; Fluorescence correlation spectroscopy; Nuclear hormone receptor; Hormone response elements; Biochemical annotation

1. Introduction

One-third of the 48 nuclear hormone receptors (NHRs) found on the human genome are orphan receptors as their ligands are not known [1]. The NHR superfamily of transcription factors directly activates or represses target genes by binding to the hormone response elements (HREs). Thus, these proteins play a central role in many biological processes such as cell growth and differentiation, embryonic development, and metabolic homeostasis in metazoan organisms. The HREs, in which a 6-bp long sequence constitutes the core recognition motif, are located in the regulatory region of the gene. Although some monomeric receptors can bind to a single hexameric recognition motif, most receptors bind as homodimers or heterodimers to the HREs composed typically of two core hexameric motifs. For dimeric HREs, the half-sites can be configured as direct repeats (DR) or as palindromes (Pal). The binding specificity of the NHR varies depending on the length of the spacer region between the two HRE half-sites [2].

Fluorescence correlation spectroscopy (FCS) is an advanced technology that is used for measuring the translational diffusion coefficients of molecules in solutions [3,4]. FCS technology is ideal for measuring the molecular interactions because the translational diffusion coefficient of a molecule depends on its molecular weight, structure and number. We recently developed an automated FCS system suitable for applications ranging from the high-throughput analyses to complex studies of molecular interactions, and using this system we have previously described a binding assay for the DNA-transcriptional factors such as NF-κB in crude cellular extracts [5]. In contrast to the electrophoretic mobility shift assay (EMSA), the binding assay using the FCS technique contained steps that are less time consuming, and consequently, the measurements can be carried out within a very short period of time (10–20 s per sample). Thus, an assay based on FCS could facilitate the analysis of DNA–protein interactions tens of times faster than EMSA.

Wheat germ extract cell-free protein synthesis technology has made it possible to produce a wide range of difficult-to-express proteins, which includes prokaryotic, eukaryotic and artificial proteins, in naturally folded states [6]. We developed a high-throughput, genome-scale protein synthesis method based on the wheat germ extract cell-free expression system, and using this system we have successfully synthesized 34 different types of human NHRs. We report here a comprehensive method for the biochemical analysis of binding between 34 different human NHRs and 12 different DNA response elements. In addition, this analysis reveals instances of new heterodimeric bindings of the NHRs.

2. Materials and methods

2.1. General

Details of the following procedures have been either described or cited previously [6,7]: generation of DNA template by PCR using split-primers, synthesis of mRNA, protein synthesis in parallel, estimation of amount of protein synthesized by means of densitometric scanning of the Coomassie brilliant blue® (CBB)-stained band and autoradiography. The wheat germ extract was purchased from Cell-Free Sciences, Co. (Yokohama, Japan). Autoradiography was analyzed by BAS-2500 (Fuji film, Tokyo, Japan). Reagents used in this study were described previously [6].

*Corresponding authors. Address: Cell-Free Science and Technology Research Center, Venture Business Laboratory, Ehime University, 3 Bunkyo-cho, Matsuyama, Ehime 790-8577, Japan. Fax: +81 89 927 9941 (T. Sawasaki).
E-mail addresses: yendo@eng.ehime-u.ac.jp (Y. Endo), sawasaki@eng.ehime-u.ac.jp (T. Sawasaki).

0014-5793/$34.00
doi:10.1016/j.febslet.2008.07.003

2.2. DNA-template construction for transcription

The DNA templates for transcription were obtained by using the split primer PCR technique using gene specific primers (S1-sense primer shown in Supplementary Table S1). PCR conditions and transcription were described previously [6].

2.3. Cell-free translation

Cell-free translation is based on a bilayer diffusion system that consists of a translation mixture and substrate mixture [7] including 10 μM zinc acetate. The translation reaction was carried out in 96-well titer plates. Each well containing 25 μl of the translation mixture was then carefully overlaid with 125 μl of the substrate mixture. The plate was incubated at 26 °C for 18 h.

2.4. Preparation of the double-stranded DNA

Sequences of the single-stranded DNAs used in this study are listed in Supplementary Table S2. Each DNA fragment was amplified with the common primer labeled with TAMRA and one of the non-labeled primers using the Ampli-Taq Gold kit. The PCR products were electrophoresed in 15% polyacrylamide, and the target TAMRA-labeled double-stranded DNA was excised from the gel and purified with QIAquick extraction kit (Qiagen, Düsseldorf, Germany). For natural response elements, the double-stranded DNA was prepared by annealing both oligonucleotides in 10 mM TE buffer (pH 8.0) containing 0.1 M sodium chloride. The reaction mixture was hydrolyzed stepwise in the $3' \rightarrow 5'$ direction by exonuclease I to remove the single-strand DNA and then the hydrolyzed nucleotides, free dyes, and salts were removed by using MERmaid SPIN (Qbiogen, Carlsbad, CA).

2.5. DNA-binding assay using the fluorescence correlation spectroscopy (FCS)

For detecting NHR–HRE binding, 5 μl of the translational mixture, including the synthesized protein product, was incubated at 30 °C for 30 min in the presence of 1 nM of TAMRA-labeled DNA. The reaction was carried out in a total volume of 24 μl reaction mixture containing 50 mM KCl, 2 mM $MgCl_2$, 20 mM Hepes-KOH (pH 7.8), 1 mM DTT, 0.1 mM EDTA, 100 μg/ml BSA, 5% glycerol and 0.2 mg/ml poly(dI–dC). The samples were sequentially and automatically loaded onto a 384-well glass-bottomed microplate, and FCS measurements were performed using the single-molecule fluorescence detection system, MF20 (Olympus, Tokyo, Japan). For hormone-dependent glucocorticoid receptor (GR) binding, synthesized GR (15 μl) was incubated with or without 5 nM cortisol at 30 °C for 30 min. For heterodimerization, 2.5 μl of retinoid X receptor (RXR) γ was mixed with 2.5 μl of vitamin D receptor (VDR), peroxisome proliferator-activated receptor (PPAR) α, PPARβ, or PPARγ. Fluorescence was measured using a He–Ne laser (excitation wavelength 543 nm) and a 580DF30 filter. The optical system of the device was automatically adjusted for each measurement. All experiments were performed under identical conditions with a data acquisition time of 15 s per measurement, and were repeated five times per sample.

2.6. Definition of positive DNA-binding ability for NHR

In the FCS assay, the diffusion time of a labeled molecule in a laser-illuminated region is measured. The diffusion time of a molecule can be theoretically calculated from its molecular weight. Here, DNA is assumed to conform to a spherical shape and its molecular weight is calculated according to 662 Da per base-pair; moreover, under saturated conditions, all the TAMRA-labeled DNA in the reaction solution is assumed to form a monomer or dimer. The diffusion time correlates with the molecular weight of the labeled molecule. When NHR binds to labeled DNA, the molecular weight of the NHR–DNA complex becomes higher than the DNA alone. In general, because the mobility of a molecule in solution dependents on its molecular weight, the mobility of the NHR–DNA complex becomes slower than DNA alone. Consequently, the slower protein–DNA complex exhibits longer diffusion time [5].

In the FCS system, therefore, NHR binding to DNA can be detected by prolonged diffusion times. This time difference is also calculated from the molecular weights of DNA and NHR complexes, assuming that each NHR forms a monomer on the core motif and forms a homodimer on DR or Pal. By comparing the results of the FCS analysis with those derived from EMSA measurements carried out in parallel, we observed that the DNA–NHR complexes were actually detected in EMSA when the prolongation of diffusion time is 30% or higher than the theoretical values. Consequently, we selected a threshold value for the binding degree, and defined the DNA-binding ability of an NHR as positive when the binding degree for the pair was 30% or higher. From a total of 408 possible binding combinations, 145 demonstrated positive binding by EMSA, whereas 140 were positive (i.e., exhibiting a binding degree 30% or higher than the threshold) by FCS.

Other materials and methods used are described in the supplementary data.

3. Results and discussion

3.1. Binding of NHRs produced by the wheat cell-free system to human natural response elements using FCS

To investigate whether NHRs synthesized by the wheat cell-free system can bind human natural response elements, we prepared the human natural response elements of apolipoprotein A-I (ApoA-I) [8] and medium-chain acyl coenzyme A dehydrogenase (MCAD) genes [9] by annealing the respective synthetic oligonucleotides (DNA sequences listed in Supplementary Table S3). ApoA-I is a major protein component of high-density lipoprotein (HDL), and plays an important role in the reverse cholesterol transport pathway. The regulatory element (−220/−190) on the ApoA-I gene contains DR of the PuGTTCA motif separated by 2 bp, and is recognized by the RXRα homodimer and RXRα/retinoic acid receptor (RAR) α heterodimer [8].

Using the FCS assay system we confirmed the binding of RXRα to the ApoA-I regulatory element, but not to the thyroid hormone receptor (TR) α regulatory element (a negative control) (Fig. 1A). Nuclear receptor response element (NRRE)-1 (−341/−307), a pleiotropic element present in the MCAD gene promoter [9], is known to interact with a number of NHRs including the RXR and estrogen related receptor (ERR). Maehara et al. previously reported that the ERR, but not the PPAR, bound to the NRRE-1 as a homodimer or as two independent monomers [10]. Consistent with this report, we also found that the ERRγ bound to the NRRE-1, whereas the PPARα (a negative control) did not (Fig. 1B).

To elucidate the hormone-mediated transcriptional network, it is important to investigate the ligand-binding as well as the DNA-binding specificities of the NHRs. We therefore examined the effects of the ligand on DNA–GR binding, finding that binding of GR to the cytochrome P450 2C9 (CYP2C9) gene promoter element was enhanced by cortisol as one of the glucocorticoids (Fig. 1C). In this way, FCS is able to contribute to the analysis of not only the NHR–HRE molecular interactions but also the ligand-NHR or DNA–NHR-ligand molecular interactions. These results suggest that the high-throughput method described here could be used to identify the natural response elements found in the promoters and enhancers, and to screen the hormone ligand to further investigate the effects on the DNA binding. Moreover, FCS represents a potentially general technique for drug selection, to identify candidates that interfere with or modify particular binding interactions.

3.2. Production of 34 human NHR proteins by the wheat germ extract cell-free system

Thirty-four NHR proteins were synthesized using the wheat germ extract cell-free system supplement with zinc ion. The

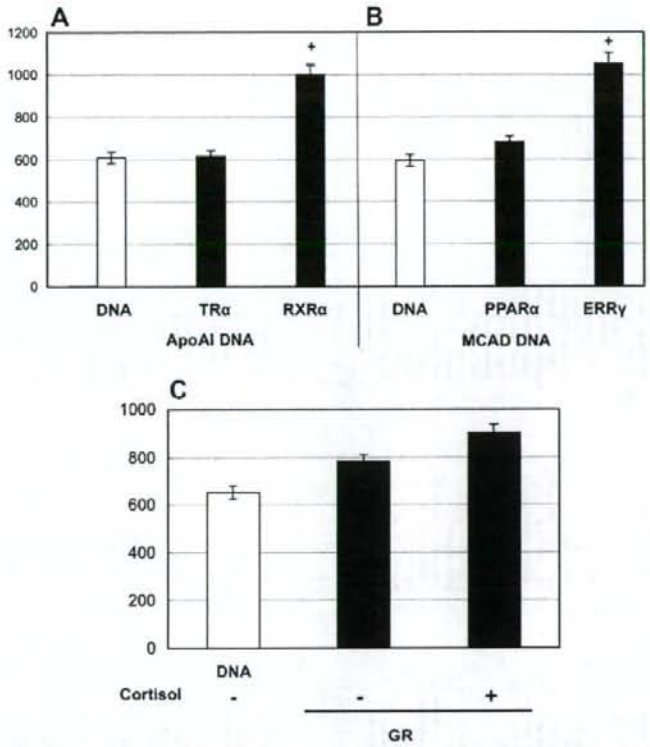

Fig. 1. FCS detection of DNA-binding specificities of RXRα and ERRγ, and hormone response of GR to the natural human DNA response elements. Binding of (A) TRα (negative control) or RXRα to the binding element on the ApoA-I gene, and (B) PPARα (negative control) or ERRγ to the binding element on the MCAD gene were examined by FCS. Binding experiments were performed using either of the synthesized protein products. The symbol "+" represents a diffusion time ratio of 30% and higher. (C) Binding of GR to the CYP2C9 gene promoter element was enhanced by cortisol as one of the glucocorticoids. The vertical axis shows the diffusion time (μs) of TAMRA-labeled DNA (1 nM) or NHR–HRE complexes in the reaction solution. Error bars represent the S.D. of five measurements.

NHR products, synthesized in the presence of radioisotope-labeled amino acid (^{14}C-Leu), were confirmed by analyzing autoradiographs of the respective SDS–polyacrylamide gels following electrophoresis. Each protein appeared as a single band on the autoradiogram (data not shown). Proteins were quantified by incorporation of ^{14}C-Leu, and the average yield was found to be approximately 3.5 ± 1.4 μg of protein per 100 μl of reaction mixture. We also checked the solubility of the each product as previously reported [7], and found that 65 ± 25% each product was soluble. The yields and solubilities of each synthesized protein are shown in Supplementary Table S4.

3.3. Binding analysis of 34 human NHRs to core, DR and Pal motifs using FCS

We used the automated FCS technique to systematically study the DNA-binding properties of 34 NHRs. In this binding assay, a given NHR protein product was mixed with a fluorescence-labeled DNA probe. Diffusion time of the labeled DNA in the reaction mixture was measured using FCS. Prolongation of diffusion time in reaction solution, compared with the control value, indicates NHR–HRE complex formation. Each diffusion time was categorized into 10 different levels (from 1 to 10) according to its binding degree, i.e. the ratio of the actual measurement value to the theoretically expected value (see Section 2.6). The double-stranded DNAs used as probes are listed in Supplementary Table S2.

In addition, we analyzed the interactions between the 34 NHRs and 12 NHEs by EMSA to confirm their DNA-binding abilities. Fig. 2 includes typical EMSA results. Comparisons of the results obtained from the FCS and EMSA analyses suggested that the NHR–HRE pairs whose diffusion times belonged to the scored categories 4 through 10, as determined from the FCS analysis, formed NHR–HRE complexes on EMSA. In contrast, the NHR–HRE pairs whose diffusion times belonged to the categories 1 through 3 as determined from FCS failed to form NHR–HRE complexes on EMSA. Thus, we determined that a diffusion time ratio of 30% and higher by FCS analysis indicates positive NHR–HRE binding.

3.4. Evaluation of NHR–HRE binding data

Table 1 summarizes the binding results of the 34 NHRs as shown in Fig. 2. Twenty-four out of thirty-four different NHRs bound to a DNA element in a ligand-independent manner. Several NHRs, such as Rev-erbAβ and tailless nuclear hormone receptor (TLX), bound to DNA only when higher amounts (15 μl) of the synthesized protein was used in the as-

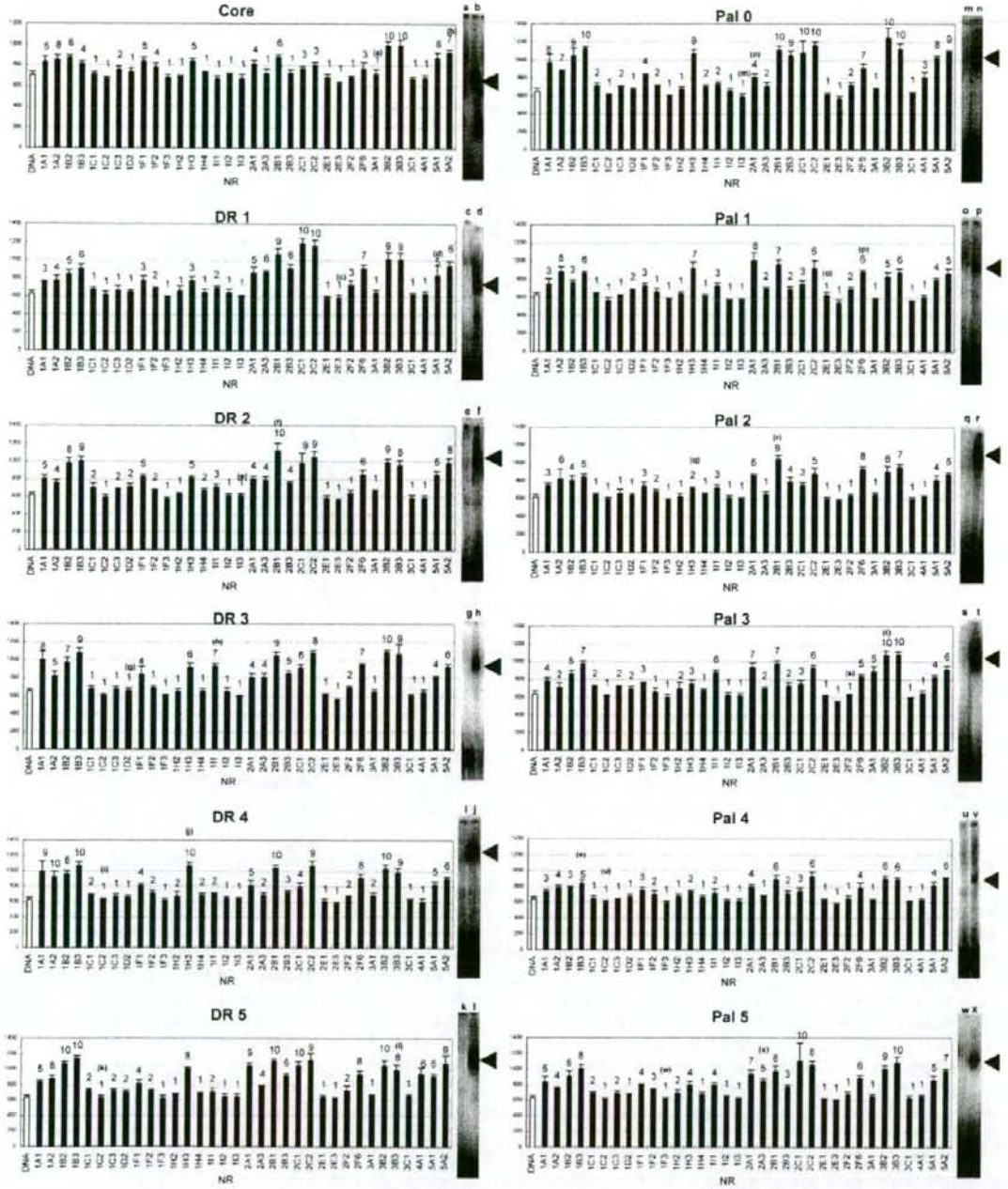

Fig. 2. Detection of NHR–HRE interactions with FCS. The vertical axis shows diffusion time (μs) of the TAMRA-labeled DNA or NHR–HRE complex in the reaction solution. Results from the representative EMSA experiments were also shown (autoradiograms). Numbers in the parentheses correspond to the representative EMSAs. Arrowheads indicate specific NHR–HRE complexes. Open bar indicates a negative control where the synthesized protein product was prepared from the plasmid lacking the DNA-binding domain. Error bars represent the S.D. over five measurements. Labels 1 through 10 indicate the diffusion time ratios of the actual measurement values to the theoretically expected values: 1 indicates less than 10%, and 2, >10–20%; 3, >20–30%; 4, >30–40%; 5, >40–50%; 6, >50–60%; 7, >60–70%; 8, >70–80%; 9, >80–90%; and 10, >90%. Core, DR and Pal indicate the DNA probes used in this experiment.

Table 1
NHR–HRE binding profiling by wheat cell-free based FCS

Genes	Names	Core	DR 1	DR 2	DR 3	DR 4	DR 5	Pal 0	Pal 1	Pal 2	Pal 3	Pal 4	Pal 5
NR1A1	TRα	+*	-	+*	+*	+*	+*	+*	-	-	+*	-	+*
NR1A2	TRβ	+*	+	+*	+*	+*	+*	+*	+	+	+*	+	+
NR1B2	RARβ	+*	+	+*	+	+	+*	+*	-	+	+*	-	+
NR1B3	RARγ	+*	+	+	+	+	+	+	+	+	+*	+	+
NR1C1	PPARα	-	-*	-	-	-	-	-	-	-	-	-	-
NR1C2	PPARβ	-	-	-	-	-	-	-	-	-	-	-	-
NR1C3	PPARγ	-	-	-	-	-	-	-	-	-	-*	-	-
NR1D2	Rev-erbAβ	-*	-	+*	-	-	-	(+)	(+)	-	(+)	(+)	-
NR1F1	RORα	+*	(+)*	+*	+	+	+	+*	(+)	(+)	(+)	(+)	+
NR1F2	RORβ	+	-	-	-	-	-	-	-	-	-	-	-
NR1F3	RORγ	-	-	-	-	-	-	-	-	-	-	-	-
NR1H2	LXRβ	-	-	-	-	-	-	-	-	-	-	-	-
NR1H3	LXRα	+	-	+	+	+*	+	+	+	-	-	-	+
NR1H4	FXR	-	-	-	-	-	-	-	-	-	-	-	-
NR1I1	VDR	-	-	-	+*	-*	(+)*	(+)	-	(+)	+	-	+
NR1I2	PXR	-	-	-	-	-	-	-	-	-	-	-	-
NR1I3	CAR	-	-	-	-	-	-	-	-	-	-	-	-
NR2A1	HNF4α	+*	+*	+*	+	+	+	+	+	+	+	+	+
NR2A3	HNF4γ	-	+	+	+	(+)	+	-	(+)	-	-	-	+
NR2B1	RXRα	+	+*	+*	+*	+*	+*	+*	+*	+*	+*	+*	+*
NR2B3	RXRγ	-	+	+	+	-*	+	+	-	(+)	-	-	(+)
NR2C1	TR2	(+)	+*	+*	+*	+*	+*	+	(+)	-	(+)	-	+
NR2C2	TR4	(+)	+*	+*	+*	+*	+*	+	+	+	+*	+	+
NR2E1	TLX	-	-	-	-	-	-	-	(+)	-	-	-	(+)
NR2E3	PNR	-	-	-	-	-	-	-	-	-	-	-	-
NR2F2	COUP-TFII	-	(+)*	(+)*	(+)*	(+)*	(+)*	(+)*	(+)*	-	-	-	-
NR2F6	EAR2	-	+*	+	+	+*	+	+*	+	+	+	-	+
NR3A1	ERα	-	-	-	-	-	-	-*	-	-	+*	-	-
NR3B2	ERRβ	+*	+	+	+	+	+	+	+	+	+	+	+
NR3B3	ERRγ	+*	+	+	+	+	+	+	+	+	+	+	+
NR3C1	GR	-	-	-	-	-	-	-	-	-	-	-	-
NR4A1	NGFI-Bα	-*	-	-	-	-	+	(+)	-	-	-	-	-
NR5A1	SF-1	+*	+	+	+	+	+	+	+	+	+	+	+
NR5A2	LRH-1	+*	+	+	+	+	+	+	+	+	+	+	+

Five μl of synthesized protein was used in this binding assay. The symbols "+" and "−" over the theoretically expected value calculated from the estimated molecular mass of the DNA–NHR complex under saturated condition where all TAMRA-labeled oligonucleotides were bound to the NHR of 30% and higher, and less than 30%, respectively. (+) Symbol in the parentheses indicates that while there was no measurable DNA–NHR interaction using 5 μl of the synthesized protein, a DNA–NHR interaction was observed when 15 μl of the synthesized protein was used in the reaction mixture. Asterisks (*) represent DNA–NHR interactions which were previously reported and the numbers refer to the respective references in the Supplementary data.

say, suggesting they have low DNA binding affinities. We examined 408 different NHR–HRE combinations (monomers and/or homodimers) for binding using the FCS-based assay, and consequently identified 205 different NHR–HRE interactions, 124 of which were novel and 81 that were previously reported (Table 1). However, eight previously reported NHR–HRE interactions (TRα-Pal4, PPARα-DR1, PPARγ-Pal3, Rev-erbAβ-core, VDR-DR4, RXRγ-DR4, ERα-Pal0, and NGFI-Bα-core) were not among the 205 NHR–HRE interactions reported in this study. One possible explanation for this discrepancy is that these eight interactions have used slightly different DNA fragments in the flanking and spacer sequences although the core sequence is the same. Because the significance of sequences around the core region is known [11,12], the interactions may also recognize flanking and/or spacer sequences in DNA fragment used.

The second explanation for the observed difference might lie in the requirement of a co-factor or ligand dependency. Almost all the previously reported NHR–HRE binding assays were performed using animal-derived protein expression systems such as rabbit reticulocyte lysate (PPARα), baculovirus-infected insect cell lysate (PPARγ and RXRγ) or cultured mammalian cell lysates (Rev-erbAβ, VDR, ERα, and NGFI-Bα). Although orphan receptors such as Rev-erbAβ and NGFI-Bα also exist among these eight combinations, these cell lysates might contain ligands and/or other essential factors for their DNA binding. This possibility is least likely in our assay system however, because the wheat germ extract is obviously of plant origin.

A third reason might be due to the nature of the protein (e.g., partial DNA-binding domain, full-length, and glutathione *S*-transferase- or FLAG-tagged proteins) used in the binding assay. Mader et al. reported that the DNA-binding domain of TR bound to the DR2 and Pal4 although the full-length TR did not bind to either DNA element [13]. We have also found that the full-length TRα did not bind to the Pal4 in our assay (Fig. 2), an observation that is consistent with that of Mader et al. In previous reports, FLAG- and HA-tagged proteins were used in the binding assay of PPARγ [11] and ERα [5], respectively. Because a full-length and non-tagged NHR protein is the original form in the cell, we believe that our assay (using a library of full-length NHRs) will provide more useful information than currently available assay systems for studying the NHR–HRE interaction.

3.5. Screening of binding partner forming heterodimers with RXRγ

RXRs are known to be promiscuous dimerization partners for a large number of NHRs, and their dimerization partners include themselves, RAR, VDR, TR, PPAR and other orphan receptors [1]. We next screened for binding of RXRγ heterodimers to DR4 and Pal3. To examine whether RXRγ heterodimerizes with VDR, PPARα, PPARβ and PPARγ, equal amounts of synthesized RXRγ and one of the four NHRs (VDR, PPARα, PPARβ or PPARγ) were mixed with each test DNA element and analyzed by FCS. We found that RXRγ heterodimerized with VDR on both DR4 and Pal3 (Fig. 3A and B). Yen et al. previously demonstrated RXR/VDR heterodimerization on DR4 [14], but RXR/VDR heterodimerization on Pal3 is a new finding. Our study also showed that the VDR bound to Pal3 as a homodimer (Fig. 3B, see also Fig. 2 and Table 1). Therefore, it is possible that the mixture of RXRγ and

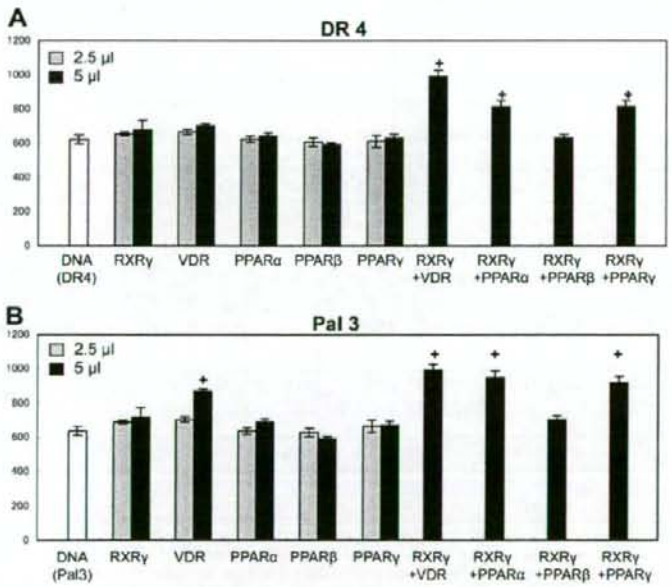

Fig. 3. DNA-binding abilities of the RXRγ/VDR, RXRγ/PPARα, RXRγ/PPARβ and RXRγ/PPARγ heterodimers. Binding of the RXRγ/VDR, RXRγ/PPARβ and RXRγ/PPARγ heterodimers with (A) DR4 and (B) Pal3 were examined by FCS. The vertical axis shows the diffusion time (μs) of the TAMRA-labeled HRE or NHR–HRE complex in the reaction solution. The symbol "+" represents a diffusion time ratio of 30% and higher. Error bars represent the S.D. of four measurements.

VDR might be forming both RXRγ/VDR heterodimers and VDR homodimers on Pal3.

In a systematic binding study using the DR elements with various spacers (DR0–DR5), it was previously shown that the RXR/PPAR heterodimer bound with the highest affinity to DR1 and with lesser affinities to DR0 and DR2 [15]. In addition, Okuno et al. reported that the RXR/PPARγ heterodimer bound to Pal3 [11]. In the present study, we found that RXRγ formed heterodimers with PPARα and PPARγ not only on Pal3 but also on DR4. However, our results showed that the RXRγ did not form a heterodimer with PPARβ on either DR4 or Pal3. Although PPARα and PPARγ did not bind to any DNA element as a homodimer (Fig. 2 and Table 1), they were able to recognize DNA sequences by forming heterodimers with RXRγ. Like PPARα and PPARγ, VDR was able to bind to DR4 as a VDR/RXR heterodimer, but not as a VDR homodimer.

3.6. Biochemical classification of human NHRs by DNA-binding profiling

We examined 408 different combinations for binding between DNA and NHRs (monomers and/or homodimers), and consequently detected 205 binding combinations of which 124 are new and 81 reported previously (Table 1). Based on the results of our binding assay, we classified all 34 NHRs into four groups (Fig. 4): (A) NHRs bound to all of the tested DNA elements with AGGTCA sequence (group A), (B) NHRs bound to two or more DR and/or Pal DNA elements (group B), (C) NHRs bound to only one type of DNA element (group C), and (D) NHRs not bound to any one of the DNA elements tested (group D). The NHRs belonging to group B were further classified into sub-groups based on their binding specificities to Core, DR and Pal (Fig. 4B-1, -2 and -3, respectively). Even though the NHRs in group D did not bind any of the tested DNA elements, several were able to form heterodimers with RXR or other receptors as described above. Although GR did not bind to any of the 12 DNA elements used in this study, it did bind to its response region in the human natural element (Fig. 1C) in our assay. Thus, we believe that some of the group D NHRs may recognize other HREs.

We compared these DNA-binding specificity-based clusters with the conventional sequence/domain conservation-based clusters. We found that the DNA sequences and the binding specificities of the group A members ERRβ and steroidogenic factor-1 (SF-1) were similar to the ERRγ and liver receptor homolog-1 (LRH-1), respectively. But, the DNA sequences of ERRβ (or ERRγ) are quite different from that of the SF-1 (or LRH-1) regardless of their similar binding specificities. Thus, our biochemical classification showed that similarity in the DNA sequence does not necessarily mean similarity in DNA-binding specificity. This approach, which categorizes NHRs in different clusters (clusters are separated by bold lines in Fig. 4), could bring new perspectives to NHRs, as the classification of the NHRs based on their DNA-binding specificities and not on their conserved sequences and/or domains. For example, our results suggest that the group A NHRs may be involved in regulating the same gene even though they bind to different hormones.

In conclusion, we propose that the combination of the high-throughput, genome-scale protein production method based

A Group A Binding to all the DNA elements with AGGTCA

Nuclear receptor	Core	DR1	DR2	DR3	DR4	DR5	Pal0	Pal1	Pal2	Pal3	Pal4	Pal5
1A2 TRβ	○	○	○	○	○	○	○	○	○	○	○	○
1B3 RARγ	○	○	○	○	○	○	○	○	○	○	○	○
1F1 RORα	●	●	●	●	●	●	●	●	●	●	●	●
2A1 HNF4α	○	○	○	○	○	○	○	○	○	○	○	○
2B1 RXRα	○	○	○	○	○	○	○	○	○	○	○	○
2C2 TR4	○	○	○	○	○	○	○	○	○	○	○	○
3B2 ERRβ	●	●	●	●	●	●	●	●	●	●	●	●
3B3 ERRγ	●	●	●	●	●	●	●	●	●	●	●	●
5A1 SF-1	○	○	○	○	○	○	○	○	○	○	○	○
5A2 LRH-1	○	○	○	○	○	○	○	○	○	○	○	○

C Group C Binding to the only one element

Nuclear receptor	Core	DR1	DR2	DR3	DR4	DR5	Pal0	Pal1	Pal2	Pal3	Pal4	Pal5
1F2 RORβ	●											
3A1 ERα										○		

D Group D Not binding to any DNA elements

Nuclear receptor	Core	DR1	DR2	DR3	DR4	DR5	Pal0	Pal1	Pal2	Pal3	Pal4	Pal5
1C1 PPARα												
1C2 PPARβ												
1C3 PPARγ												
1F3 RORγ												
1H2 LXRβ												
1H4 FXR												
1I2 PXR												
1I3 CAR												
2E3 PNR												
3C1 GR												

B Group B Binding to two and more core, DR and /or Pal elements

1) Core

Nuclear receptor	Core
1A1 TRα	○
1B2 RARβ	○
1H3 LXRα	○
2C1 TR2	○
1D2 Rev-erbAβ	
1I1 VDR	
2A3 HNF4γ	
2B3 RXRγ	
2E1 TLX	
2F2 COUP-TFII	
2F6 EAR2	
4A1 NGFI-Bα	

2) DR

Nuclear receptor	DR 1	DR 2	DR 3	DR 4	DR 5
1B2 RARβ	○	○	○	○	○
2C1 TR2	○	○	○	○	○
2F2 COUP-TFII	○	○	○	○	○
2F6 EAR2	○	○	○	○	○
2A3 HNF4γ	○	○	○	○	○
1A1 TRα		○	○	○	○
1H3 LXRα		○	○	○	○
2B3 RXRγ	○	○	○		○
1D2 Rev-erbAβ		●			
1I1 VDR			○		○
2E1 TLX					
4A1 NGFI-Bα					●

3) Pal

Nuclear receptor	Pal0	Pal1	Pal2	Pal3	Pal4	Pal5
1H3 LXRα	○	○				○
2F2 COUP-TFII	○	○				
1D2 Rev-erbAβ	●	●		●	●	
2C1 TR2	○	○		○		○
1I1 VDR	○		○	○		○
1B2 RARβ	○		○	○		○
1A1 TRα	○			○		○
2A3 HNF4γ		○				○
2E1 TLX		○				○
2B3 RXRγ	○		○			○
2F6 EAR2	○	○	○	○		○
4A1 NGFI-Bα	●					

Fig. 4. Biochemical classification of human NHRs based on NHR–HRE binding specificities. Out of 34 synthesized NHRs, 24 bound to various DNA test elements. Thirty-four NHRs were divided into four groups on the basis on their binding specificities: (A) NHRs bound to all of the tested DNA elements with AGGTCA sequence (group A), (B) NHRs bound to two or more Core, DR and/or Pal DNA elements (group B), (C) NHRs bound specifically to only one type of DNA element (group C), and (D) NHRs not bound to any one of the tested DNA elements (group D). A positive NHR–HRE interaction is indicated with a colored circle (filled). Blank boxes in group D indicate that the NHRs listed did not interact with the Core, DR or Pal DNA element. NHRs having same or very similar DNA-binding activities are boxed in bold lines.

on the wheat germ extract cell-free expression system and the automated FCS technique offers a favorable methodology for the functional analysis of DNA–protein interactions. We also believe that the novel biochemical classification method described in this study might help in obtaining knowledge important for elucidating the NHR mediated-transcriptional network.

Further discussion is included in the supplementary data.

Acknowledgement: This work was partially supported by the Special Coordination Funds for Promoting Science and Technology by the Ministry of Education, Culture, Sports, Science and Technology, Japan (T.S. and Y.E.).

Appendix A. Supplementary data

Supplementary data associated with this article can be found, in the online version, at doi:10.1016/j.febslet.2008.07.003.

References

[1] Aranda, A. and Pascual, A. (2001) Nuclear hormone receptors gene expression. Physiol. Rev. 81, 1269–1304.
[2] Khorasanizadeh, S. and Rastinejad, F. (2001) Nuclear–receptor interactions on DNA-response elements. Trends Biochem. Sci. 26, 384–390.
[3] Ehrenberg, M., Cronvall, E. and Rigler, R. (1971) Fluorescence of proteins interacting with nucleic acids Correction for light absorption. FEBS Lett. 18, 199–203.
[4] Wolcke, J., Reimann, M., Klumpp, M., Göhler, T., Kim, E. and Deppert, W. (2003) Analysis of p53 "latency" and "activation" by fluorescence correlation spectroscopy Evidence for different modes of high affinity DNA binding. J. Biol. Chem. 278, 32587–32595.
[5] Kobayashi, T., Okamoto, N., Sawasaki, T. and Endo, Y. (2004) Detection of protein–DNA interactions in crude cellular extracts by fluorescence correlation spectroscopy. Anal. Biochem. 332, 58–66.
[6] Sawasaki, T., Ogasawara, T., Morishita, R. and Endo, Y. (2002) A cell-free protein synthesis system for high-throughput proteomics. Proc. Natl. Acad. Sci. USA 99, 14652–14657.
[7] Sawasaki, T., Hasegawa, Y., Tsuchimochi, M., Kamura, N., Ogasawara, T., Kuroita, T. and Endo, Y. (2002) A bilayer cell-free protein synthesis system for high-throughput screening of gene products. FEBS Lett. 514, 102–105.
[8] Mader, S., Leroy, P., Chen, J.Y. and Chambon, P. (1993) Multiple parameters control the selectivity of nuclear receptors for their response elements selectivity and promiscuity in response element recognition by retinoic acid receptors and retinoid X receptors. J. Biol. Chem. 268, 591–600.
[9] Carter, M.E., Gulick, T., Moore, D.D. and Kelly, D.P. (1994) A pleiotropic element in the medium-chain acyl coenzyme A dehydrogenase gene promoter mediates transcriptional regulation by multiple nuclear receptor transcription factors and defines novel receptor-DNA binding motifs. Mol. Cell. Biol. 14, 4360–4372.
[10] Maehara, K., Hida, T., Abe, Y., Koga, A., Ota, K. and Kutoh, E. (2003) Functional interference between estrogen-related receptor alpha and peroxisome proliferator-activated receptor alpha/9-cis-retinoic acid receptor alpha heterodimer complex in the nuclear receptor response element-1 of the medium chain acyl-coenzyme A dehydrogenase gene. J. Mol. Endocrinol. 31, 47–60.
[11] Okuno, M., Arimoto, E., Ikenobu, Y., Nishihara, T. and Imagawa, M. (2001) Dual DNA-binding specificity of peroxisome proliferator-activated receptor gamma controlled by heterodimer formation with retinoid X receptor alpha. Biochem. J. 353, 193–198.
[12] Retnakaran, R., Flock, G. and Giguère, V. (1994) Identification of RVR, a novel orphan nuclear receptor that acts as a negative transcriptional regulator. Mol. Endocrinol. 8, 1234–1244.
[13] Mader, S., Chen, J.Y., Chen, Z., White, J., Chambon, P. and Gronemeyer, H. (1993) The patterns of binding of RAR, RXR and TR homo- and heterodimers to direct repeats are dictated by the binding specificites of the DNA binding domains. EMBO J. 12, 5029–5041.
[14] Yen, P.M., Liu, Y., Sugawara, A. and Chin, W.W. (1996) Vitamin D receptors repress basal transcription and exert dominant negative activity on triiodothyronine-mediated transcriptional activity. J. Biol. Chem. 271, 10910–10916.
[15] Kliewer, S.A., Arimoto, E., Ikenobu, Y., Nishihara, T. and Imagawa, M. (1992) Convergence of 9-cis retinoic acid and peroxisome proliferator signalling pathways through heterodimer formation of their receptors. Nature 358, 771–774.

FEBS Letters 582 (2008) 1795–1801

The wheat germ cell-free based screening of protein substrates of calcium/calmodulin-dependent protein kinase II delta

Takashi Masaoka[a], Mayuko Nishi[c], Akihide Ryo[c], Yaeta Endo[a,b,d,*], Tatsuya Sawasaki[a,b,d,*]

[a] *Cell-free Science and Technology Research Center, Ehime University, Matsuyama 790-8577, Japan*
[b] *The Venture Business Laboratory, Ehime University, Matsuyama 790-8577, Japan*
[c] *AIDS Research Center, National Institute of Infectious Diseases, 1-23-1 Toyama, Shinjuku-ku, Tokyo 162-8640, Japan*
[d] *RIKEN Genomic Sciences Center, 1-7-22 Suehiro-cho, Tsurumi, Yokohama 230-0045, Japan*

Received 22 February 2008; revised 19 March 2008; accepted 2 April 2008

Available online 16 May 2008

Edited by Jesus Avila

Abstract Calcium/calmodulin-dependent protein kinase II (CaMKII) plays a crucial role in mediating calcium signaling. Here, we demonstrate a method for screening substrates phosphorylated by human CaMKIIδ using a wheat cell-free system. The cell-free mixture expressing CaMKIIδ was incubated with HeLa extracts and radiolabeled ATP. From analysis of two-dimensional electrophoresis gels and mass spectrometry, two proteins were found. The cell-free based in vitro kinase assay revealed that CaMKIIδ phosphorylates eukaryotic translation initiation factor 4B and stress-induced phosphoprotein 1 (STIP1), the latter on Ser189. Furthermore, constitutively-active CaMKIIδ phosphorylated STIP1 in HeLa cells and dramatically promoted nuclear localization of STIP1, suggesting that calcium signals via CaMKIIδ may regulate subcellular localization of STIP1. This approach may be a useful tool for target screening of protein kinases.

Structured summary:
MINT-6538664: *CAMK2D* (uniprotkb:Q13557) *phosphorylates* (MI:0217) *STIP1* (uniprotkb:P31948) by *protein kinase assay* (MI:0424)
MINT-6538652: *CAMK2D* (uniprotkb:Q13557) *phosphorylates* (MI:0217) *EIF4B* (uniprotkb:P23588) by *protein kinase assay* (MI:0424)

*Keywords*Cell-free protein synthesis; Protein kinase; Phosphorylation; Substrate screening; Calcium/calmodulin-dependent protein kinase II; Stress-induced phosphoprotein 1

1. Introduction

Calcium, Ca^{2+}, is one of the most important signals in eukaryotic cells and induces many biochemical protein functions [1]. Multifunctional Ca^{2+}/calmodulin-dependent protein kinase II (CaMKII) is a major mediator of Ca^{2+} signaling that translates elevation of intracellular Ca^{2+} level into phosphorylation of target proteins that participate in a wide range of cellular functions including fertilization, proliferation, differentiation, learning and memory. Four isoforms (α, β, γ and δ) of CaMKII are found in mammalian genomes [2]. The γ and δ isoforms are ubiquitously expressed in most tissues, whereas the α and β isoforms are found abundantly in brain. The identification of substrate proteins of CaMKII would be useful in understanding molecular regulatory mechanisms by Ca^{2+} and phosphorylation signaling.

One of the simple biochemical approaches to identifying kinase substrates is to incubate protein kinase with cell extracts, and then to analyze the phosphorylated proteins by two-dimensional electrophoresis (2-DE) [3]. The advantage of this method is that it can screen thousands of natural substrates in the cell. However, it is often difficult to prepare sufficient functionally active kinases for the biochemical analysis because conventional recombinant protein production technologies, as represented by *Escherichia coli* cells, cannot produce those proteins that affect the physiology of the host cell. In addition, the cell-based protein production systems require the high quality purification of protein kinase for the screening because they have high phosphorylation activities of endogenous protein kinases. However, the quality control is one of the most time-consuming steps. We developed a wheat germ cell-free protein production system [4–7], and recently have successfully produced over ~400 eukaryotic protein kinases [8,9]. Furthermore, the wheat cell-free system had very low activities of endogenous protein kinases [10]. Taking advantage of this feature, we attempted to identify substrates of CaMKIIδ (CaMKIId) in HeLa cells by mixing of the HeLa cell extracts and the wheat cell-free extracts expressing CaMKIId. Two phosphorylated proteins were identified by matrix-assisted laser desorption/ionization time-of-flight mass spectrometry (MALDI-TOF-MS) after separation on 2-DE gel. Confirmation of protein phosphorylations and identification of phosphorylation site were investigated by an in vitro kinase assay based on the cell-free system. The biological significance of the phosphorylation site was substantiated by cotransfection analysis. From these studies, we have

*Corresponding authors. Address: Cell-free Science and Technology Research Center, Ehime University, Matsuyama 790-8577, Japan. Fax: +81 89 927 9941.
E-mail addresses: yendo@eng.ehime-u.ac.jp (Y. Endo), sawasaki@eng.ehime-u.ac.jp (T. Sawasaki).

Abbreviations: CaMKIId, calcium/calmodulin-dependent protein kinase II delta; DHFR, dihydrofolate reductase; 2-DE, two-dimensional gel electrophoresis; MALDI-TOF-MS, matrix-assisted laser desorption/ ionization time-of-flight mass spectrometry; bls, biotin ligation site; STIP1, stress-induced phosphoprotein 1; eIF4B, eukaryotic translation initiation factor 4B; mSTI1, murine stress-inducible protein 1; CA, constitutively active; KD, kinase dead

0014-5793/$34.00
doi:10.1016/j.febslet.2008.04.060

successfully identified stress-induced phosphoprotein 1 (STIP1) and eukaryotic translation initiation factor 4B (eIF4B) as novel substrates of CaMKIId, and also could present a simple way to identify substrates of protein kinase using the crude kinase expressed in the cell-free system.

2. Materials and methods

2.1. General

Details of the following procedures have been either described or cited previously [4–9]: generation of DNA template by PCR using split-primers, synthesis of mRNA, protein synthesis in parallel, estimation of amount of protein synthesized by means of densitometric scanning of the Coomassie brilliant blue® (CBB)-stained band and autoradiography. The wheat germ extract was purchased from CellFree Sciences Co. (Yokohama, Japan).

2.2. Plasmid construction

Three genes, CaMKIId (GenBank accession number AF071569), STIP1 (gi:5803180) and eIF4B (gi:18146613) were amplified from commercially available human cDNA (biochain, Hayward, CA) or cDNAs from HeLa cells by PCR with LA Taq polymerase (TakaraBIO, Otsu, Shiga) and primers (5′-GAGACTCGAGATGGCTTCGACCACCACCTG and 5′-GAGAGGATCCTCAGATGTTTTGCCACAAAG for CaMKIId, 5′-CCACCCACCACCACCAATGGAGCAGGTCAATGAG and 5′-TCACCGAATTGCAATCAG for STIP1, 5′-CCACCCACCACCACCAATGGCGGCCTCAGCAAAAAAG and 5′-CTATTCGGCATAATCTTCTCCC for eIF4B,), and then inserted into pT7blue vector (Merck). FLAG-STIP1 was amplified by PCR and cloned into pcDNA3.1(−)(Invitrogen). The point mutants of eIF4B (S93A, S422A, S425A, S498A, S504A, S597A), STIP1 (S189A, T198A), constitutively active (CA) CaMKIId (T287D) and kinase dead (KD) CaMKIId (T287D, K43M) were generated by PCR mutagenesis using the Quikchange mutagenesis method (Stratagene, La Jolla, CA).

2.3. Construction of transcriptional template and in vitro transcription

Construction of CaMKIId transcriptional template by split-primer PCR and in vitro transcription were performed as described [7]. Transcriptional templates of STIP1, eIF4B and their mutants were constructed in fusion forms containing a biotin ligation site (bls) at the N-terminus (that is essential for protein biotinylation) [10] using the split primer PCR method with E01-bls-S1 (5′-GGTGACACTATAGAACTCACCTATCTCTCTACACAAAACATTTCCCTACATACAACTTTCAACTTCCTATTATGGGCCTGAACGACATCTTCGAGGCCCAGAAGATCGAGTGGCACGAACTCCACCCACCACCACCAATG) primer instead of primer-2.

2.4. Wheat germ cell-free protein production

Proteins were synthesized in a dialysis cup (molecular weight cutoff 12000; Biotech International) overnight using published protocols [7]. SDS–PAGE with CBB staining was used to determine target protein yields ('total', 'soluble' and 'pellet' fractions). Synthesized CaMKIId was exchanged into phosphoreaction buffer (50 mM Tris–HCl, pH 7.5, 10 mM $MgCl_2$, 0.5 mM DTT) using G-25 spin columns (Amersham). In vitro transcription and cell-free protein synthesis based on bilayer reaction mode were performed as described [6]. The biotinylated proteins were obtained as described previously [10].

2.5. Screening of CaMKIId substrate and 2-DE

HeLa cells ($\sim 1 \times 10^7$) were harvested by centrifugation and suspended in 100 μl of extraction buffer (50 mM Tris–HCl, pH 7.5, 1 mM EDTA, 6 mM beta-mercaptoethanol). The mixture was lysed using the freeze–thaw method. After centrifugation for 15 min at $20000 \times g$ the supernatant was exchanged into phosphoreaction buffer using a G-25 spin column. HeLa cell extracts (20 μl) were pre-incubated in 7 μl of crude CaMKIId (or dihydrofolate reductase (DHFR) as a control), 100 μM ATP, 7 μl of 5× activation buffer (containing 5 mM $CaCl_2$, 5 μM calmodulin from human brain (ALEXIS corporation, Lausen, Switzerland), 0.1 mg/ml BSA) and 2 μl of 5× phosphoreaction buffer at 30 °C for 20 min. 370 kBq of [γ-^{32}P] ATP (*ICN*) was then added to the reaction mixture (35 μl of total volume) and incubated at 30 °C for 30 min. Following the reaction, proteins were separated on 2-DE gel. First-dimension isoelectric focusing was performed using pH 3–10 immobilized pH gradient (IPG) strips (Bio-Rad). IPG strips were rehydrated in rehydration buffer (9.8 M Urea, 0.5% CHAPS, 10 mM DTT) and reaction mixtures were focused at 4000 V and 25 μ A_{max}/gel for 30000 V h. After isoelectric focusing, IPG strips were washed for 5 min with equilibration buffer (6 M Urea, 2% SDS, 0.375 M Tris–HCl, pH 8.8, 20% glycerol, 130 mM DTT) four times and then IPG strips were applied to the second-dimension 12.5% SDS–PAGE. Finally, we determined which proteins were phosphorylated by gel image analysis of CBB staining and autoradiograms by BAS-2500 (FUJIFILM, Tokyo, Japan).

2.6. Identification of phosphorylated protein by MALDI-TOF-MS

After 2-DE gel image analysis, two protein spots were selected, and analyzed by peptide mass fingerprinting using MALDI-TOF-MS and database searching (MS-Fit). The peptide mass fingerprinting was performed by Promega Corporation.

2.7. In vitro phosphorylation assay

To obtain purified CaMKIId of wildtype, CA or KD form, GST-TEVsite-CaMKIId fused genes were inserted into pEU3b vector [7] and were used for the cell-free system as described above. The GST-fusion proteins were purified on Glutathione Sepharose 4B (Amersham), and then the CaMKIId proteins were recovered by on-column cleavage using AcTEV protease (Invitrogen) which cleaves at the TEVsite.

Cell-free synthesized bls-STIP1 and bls-eIF4B were biotinylated by the cell-free BirA system [10], and 20 μl of each biotinylated protein coupled to 10 μl of MagneSphere Strept beads (Promega) and incubated at 26 °C for 1 h. After incubation, protein-coupled beads were washed three times with phosphoreaction buffer and then incubated the beads with 200 ng of purified recombinant CaMKIId, 3 μl of 5× activation buffer, 3 μl of 5× phosphoreaction buffer and 37 kBq of [γ-^{32}P]ATP in a total volume of 15 μl at 30 °C for 20 min. After reaction, the beads were washed three times with 1× PBS(−), then boiled in sample buffer (50 mM Tris–HCl, pH 6.8, 2% SDS, 1% 2-mercaptoethanol, 0.004% bromophenol blue) and separated by 12% polyacrylamide gels. Phosphorylation was visualized by autoradiography.

2.8. Cell culture, transient transfections

HeLa cells were cultured in Dulbecco's modified Eagle's medium supplemented with 10% fetal bovine serum and 1% penicillin (100 mg/ml)/streptomycin (50 μg/ml). Transient transfections were carried out using Effectene Transfection Reagent (QIAGEN). Twenty-four hours after transfection, the cells were lysed and subjected to SDS–PAGE. Mobility shift detection of phosphorylated proteins was performed using phos-tag acyrylamide gel (Nard Institute Inc., Amagasaki, Japan) according to the manufacture's instruction and then analyzed by immunoblotting with anti-FLAG M2 antibodies (SIGMA).

2.9. Fluorescence imaging

HeLa cells on coverslips were transfected with FLAG-STIP1 and co-transfected with empty vector (EV), CA or KD mutants of CaMKIId using Effectene Transfection Reagent (QIAGEN), according to the manufacturer's instructions. Twenty-four hours after transfection, the cells were fixed with 3% formaldehyde and washed with PBS, and were immunostained with anti-FLAG M2 antibody (SIGMA) and then 4′,6-diamidino-2-phenylindole (DAPI). After washing with PBS, slides were visualized under a fluorescent microscope (Olympus, Tokyo, Japan) as described previously [11].

3. Results

3.1. Cell-free protein synthesis of CaMKIId and measurement of product quality

In order to assess the quality of the cell-free synthesized protein, we measured the amount, solubility and phosphorylating activity of CaMKIId. The amount and solubility of the CaMKIId as estimated from densitometric scanning of the bands

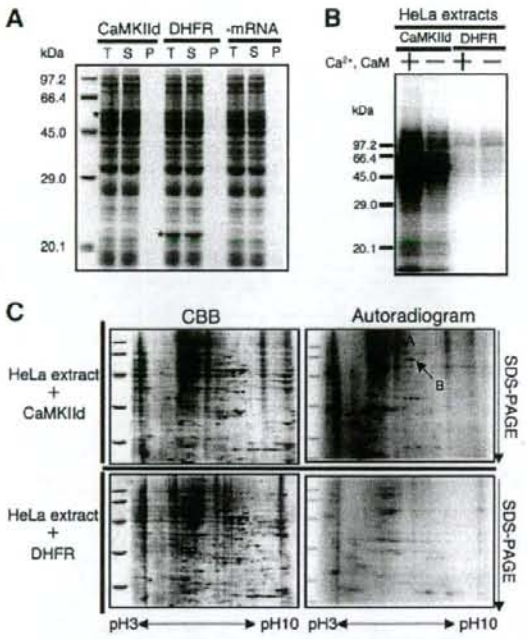

Fig. 1. Production and solubility of cell-free synthesized CaMKIId and autoradiograms of CaMKIId reactions. (A) Cell-free translation products were separated by SDS–PAGE and stained with CBB. T, S and P, respectively, mark total translation product, the supernatant fraction after centrifugation at $30000 \times g$ for 15 min and precipitate. Asterisks mark the synthesized proteins. (B) HeLa cell extracts were incubated with CaMKIId, Ca^{2+} and calmodulin at 30 °C for 20 min in the presence of [γ-^{32}P]ATP, then the reaction mixture separated by SDS–PAGE. (C) Reaction mixtures were separated by 2-DE gel and the phosphorylated proteins detected by autoradiography to determine the candidate CaMKIId substrates.

were ~200 μg/ml and ~90%, respectively (Fig. 1A). We investigated whether the wheat cell-free extract expressing CaMKIId (crude CaMKIId) could phosphorylate proteins in the HeLa cell extracts with or without Ca^{2+}/calmodulin in the presence of radiolabeled ATP. The phosphorylation was detected by autoradiography after SDS–PAGE. Protein phosphorylation in HeLa cell extracts was dramatically induced by addition of CaMKIId and Ca^{2+}/calmodulin (Fig. 1B). These results indicate that the wheat cell-free system could synthesize the CaMKIId in a folded state and that phosphorylating activity is strongly enhanced by supplementing with Ca^{2+}/calmodulin without a purification step. Interestingly four protein bands of ~90 kDa, ~64 kDa, ~50 kDa and 43 kDa were strongly phosphorylated by CaMKIId. The phosphorylating activity of CaMKIId in the absence of both Ca^{2+} and calmodulin indicates that there is partial activation by Ca^{2+}/calmodulin from HeLa cells and/or wheat germ extracts. In contrast, the addition of the wheat extract expressing DHFR (crude DHFR), as a control, had no significant influence on protein phosphorylation even in the presence of Ca^{2+}/calmodulin, indicating that the endogenous kinase activity in the wheat extract is low, and the wheat germ cell-free system is suitable for screening of substrate proteins phosphorylated by CaMKIId.

3.2. Identification of CaMKIId substrate proteins

The substrate screening was conducted by mixing crude CaMKIId with HeLa cell extracts and [γ-^{32}P] ATP followed by 2-DE gel. The total protein spots and the phosphorylated spots by CaMKIId were analyzed by gel images of CBB staining and autoradiogram, respectively (Fig. 1C). By the analysis, more than 90 phosphorylated spots were observed. Of these, 32 proteins were CaMKIId-dependently phosphorylated and 11 of them were detectable by CBB staining. Six of the 11 were derived from HeLa cell extracts. From separation quality of the CBB-staining spots, two HeLa proteins (marked in Fig. 1C) strongly phosphorylated were selected as candidate substrates and then were used for peptide mass fingerprinting by MALDI-TOF-MS. The data from each spot were submitted to MS-Fit. Seventeen and 11 of the 30 submitted ions were matched to theoretical tryptic peptides from eIF4B and STIP1, respectively (Fig. 2). The molecular weight of STIP1 and eIF4B were calculated as 62.6 and 69.1 kDa, respectively. These corresponded to the size of each spot on the 2D-gel. Although in vitro phosphorylation of STIP1 and eIF4B by some protein kinases has been reported [12–14], the two proteins are new candidate substrates of CaMKIId.

3.3. Confirmation of STIP1 and eIF4B phosphorylation

In the next step, an in vitro kinase assay was used to examine whether CaMKIId directly phosphorylates the two proteins. For this, STIP1 and eIF4B genes were cloned from cDNAs prepared from total RNA of HeLa cells, and were fused with bls at its N-terminus by split-primer PCR (see Section 2) for simple purification. After cell-free protein production, each product was biotinylated, and was purified by using streptavidin-conjugated magnetic beads. In vitro kinase assays were performed by which the purified CaMKIId and substrate proteins were incubated with radiolabeled ATP, and then confirmed direct phosphorylation of STIP1 and eIF4B by CaMKIId (Fig. 3A). The molecular weight of STIP1 and eIF4B, calculated as 62.6 and 69.1 kDa, respectively, were corresponded to the size of each spot on the 2D-gel. These data show that STIP1 and eIF4B are new in vitro substrates for CaMKIId.

3.4. Mutational analysis of STIP1 for identification of the site phosphorylated by CaMKIId

Although there is little known about the biological effect of phosphorylation of eIF4B, it is suggested that phosphorylation of Ser422 by p70S6K interferes with translation initiation in vivo[15]. A phosphorylation site in human STIP1 has been reported to be Y354 [16], but it is not known about Ser/Thr residues. However, phosphorylation on Ser189 and Thr198 has been found in its mouse homolog, murine stress-inducible protein 1 (mSTI1), and has been suggested that these two phosphorylations control nuclear transport [12]. To further understand the functions of CaMKIId with respect to the substrate proteins, we performed mutational analysis to identify the phosphorylation site(s) of STIP1 and eIF4B by CaMKIId. The Ser or Thr residues known as phosphorylation sites in STIP1 and eIF4B were mutated to alanine, and then the point mutants were used for the in vitro kinase assay. There was no effect on the phosphorylation of six eIF4B mutants (S93A, S422A, S425A, S498A, S504A, S597A, data not shown). However, the mutational analysis of STIP1 showed that Ser189 was

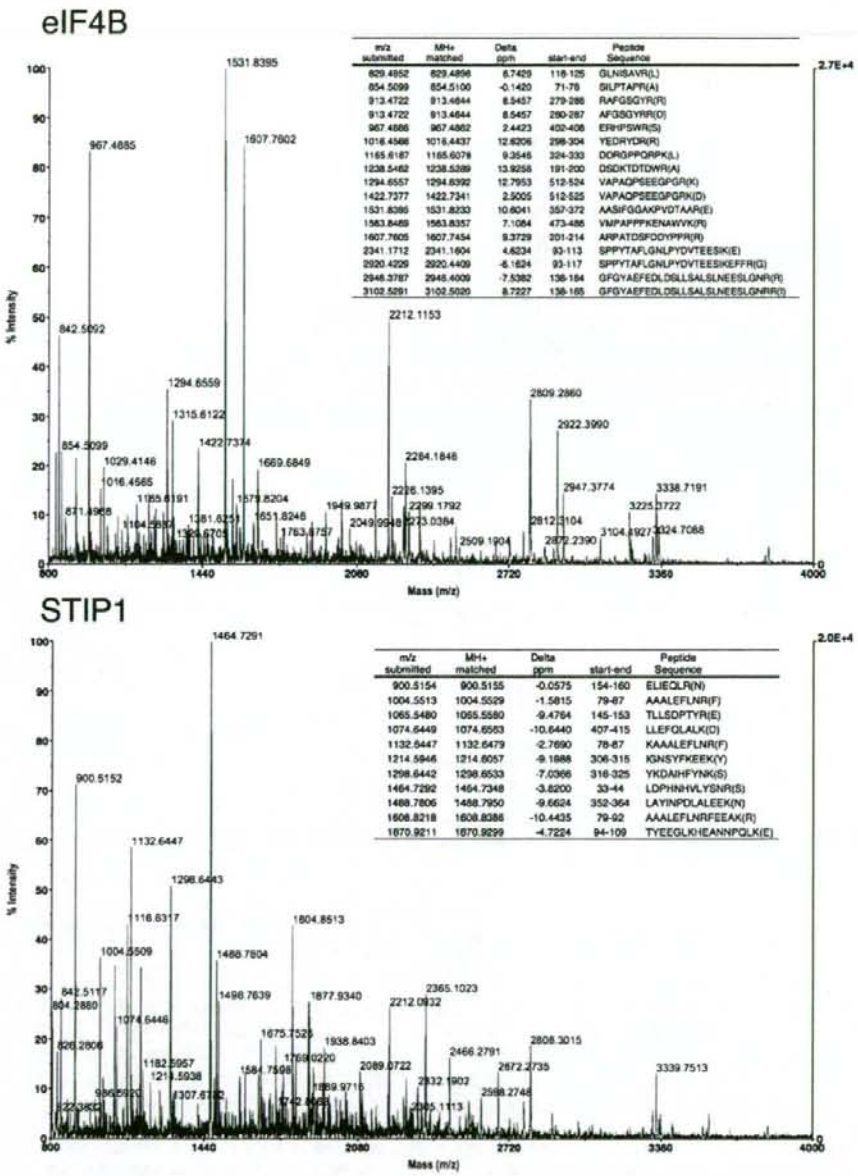

Fig. 2. MALDI-TOF-MS spectra of tryptic digests of candidate substrates. Two candidate substrate spots (A and B; indicated by arrows in Fig. 1C) were excised from 2-DE gel and were digested with trypsine. The resulting peptides were analyzed using MALDI-TOF-MS. The two candidate CaMKIId substrates were identified as STIP1 and eIF4B from the MS-Fit results.

the target residue of CaMKIId phosphorylation and T198A mutant was phosphorylated by CaMKIId (Fig. 3B).

3.5. *In vivo phosphorylation of STIP1 by CaMKIId promotes nuclear translocation*

To examine the in vivo phosphorylation of STIP1 by CaMKIId, we constructed constitutively active (CA) or kinase dead (KD) mutants of CaMKIId. The in vitro phosphorylation of STIP1 by purified CA or KD mutants showed that CA mutant phosphorylated STIP1 even in the absence of Ca^{2+}/calmodulin, whereas KD mutant had no kinase activity (Fig. 4A). We utilized the phos-tag gel system to monitor the in vivo protein phosphorylation as shifted bands [17]. HeLa cells were transfected with FLAG-STIP1 and co-transfected with empty

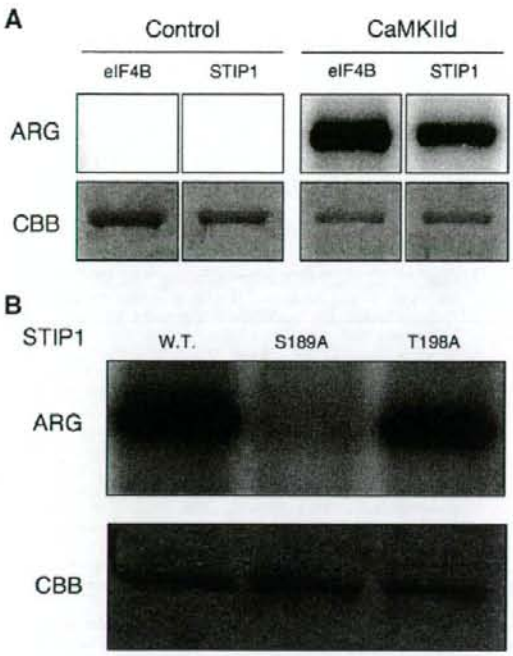

Fig. 3. In vitro kinase assay with STIP1 and eIF4B and identification of phosphorylation site on STIP1. (A) The STIP1 and eIF4B genes were cloned from HeLa cDNAs and the gene products synthesized as bls fused protein using the cell-free system. The two biotinylated proteins were purified using streptavidin-conjugated magnetic beads, then the beads were suspended in reaction mixture containing CaMKIId (or DHFR as a control), [γ-^{32}P]ATP, Ca^{2+} and calmodulin and incubated at 30 °C for 30 min. After washing, proteins were separated by 12.5% SDS–PAGE and results were visualized by autoradiography. (B) Biotinylated STIP1 mutant (S189A) was synthesized by the cell-free system and was used in the in vitro kinase assay.

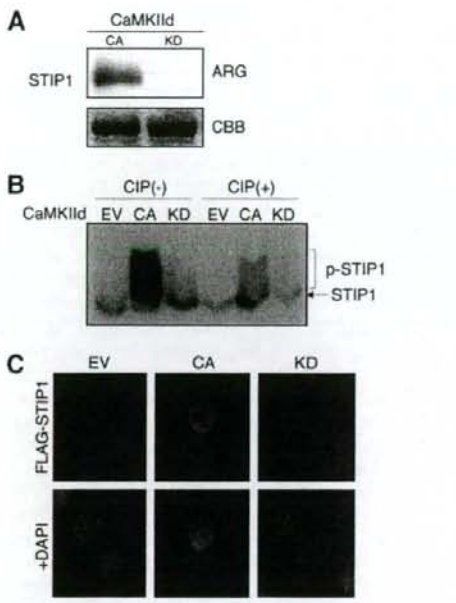

Fig. 4. In vivo phosphorylation of STIP1 and nuclear localization of STIP1 by expression of constitutively active CaMKIId. (A) Biotinylated STIP1 was purified using streptavidin-conjugated magnetic beads, then the beads were suspended in reaction mixture containing purified CA or KD CaMKIId mutants as described in Fig. 3. (B) HeLa cells were transfected with FLAG-STIP1 and co-transfected with empty vector (EV) or constitutive active (CA) or kinase dead (KD) CaMKII constructs. After 24 h, cell lysates were treated or untreated with calf intestine alkaline phosphatase (CIAP) and separated by phos-tag acrylamide gel, followed by immunoblotting with anti-FLAG antibody. (C) HeLa cells were transfected with FLAG-STIP1 and co-transfected with EV or CA or KD CaMKIId constructs. After 24 h, cells were fixed, permeabilized and immunostained with anti-FLAG (M2) antibody and subsequently stained with 4′,6-diamino-2-phenylindole (DAPI), and then subjected to fluorescent microscopy.

vector (EV) or CA or KD mutants of CaMKIId, After 24 h following transfection, cell lysates were subjected to phos-tag gel analysis. As indicated in Fig. 4B, significant band shift, indicative of phosphorylated STIP1, was observed in cells transfected with CA, but neither EV nor KD (left panel). This shift was significantly reduced when cell lysates were treated with calf intestine alkaline phosphatase (right panel), indicating that CaMKIId can phosphorylate STIP1 in vivo. We next address the biological effect of STIP1 phosphorylation by CaMKIId. Immunofluorescent analysis revealed that STIP1 is selectively localized at the nuclei in CA expressing cells, as detected by DAPI stain, while it was mainly localized in cytoplasm and cell periphery in EV or KD expressing cells (Fig. 4C). Cell viability and morphology were not significantly changed in transfected cells. The Ser189 in STIP1 was previously reported as a phosphorylation site of Casein kinase II (CKII). However, expression of EV and KD mutant showed cytoplasmic and cell-peripheral localization of STIP1 in the cell. Furthermore, treatment with specific CKII inhibitor (5,6-dichlorobenzimidazole 1-β-D-ribofuranoside) had no effect on the cytoplasmic distribution of mSTI1 [12]. Taken together, these data suggest that CKII in these cells may not be a crucial regulator of STIP1 localization to the nucleus. These results indicate that the phosphorylation of STIP1 by CaMKIId exerts the nuclear translocation of STIP1 for certain biological function.

4. Discussion

STIP1 interacts with Hsp70 and Hsp90 at its N and C termini in the cytoplasm as a co-chaperone, and can modulate the chaperone activities of these Hsps [18,19]. It is also known that STIP1 may be an important component in the oligomerization of heat-shock transcription factor (HSF1) complex in the nucleus [20]. STIP1 localizes predominantly cytoplasmic under normal growth conditions, and it might move between cytoplasm and nucleus under certain cell cycle conditions [12]. Phosphorylation of mSTI1, the mouse homologue of human STIP1, at Ser189 and Thr198 by cell cycle kinases (CKII and cdc2 in vitro, respectively) may modulate nuclear import and export in vivo [12]. In a recent report, STIP1 translocated to the nucleus in response to heat shock [21]. Interestingly, it has also been found that heat shock response was increased

concentration of the intercellular Ca^{2+} in a variety of cells [22]. These observations lead to speculation that CaMKIId might induce nuclear translocation of STIP1 in response to heat shock. In this study, we identified that the CaMKIId phosphorylated STIP1 at Ser189 in HeLa cells and also confirmed that co-transfection with CA-CaMKIId promotes STIP1 nuclear localization. The results suggest that calcium signals via CaMKIId may regulate subcellular localization of STIP1.

In the case of eIF4B, phosphorylation by S6K1, PKC, PKA, CK1, CKII and PAK1 has been reported in vitro [13,14]. The known phosphorylation sites of human eIF4B are Ser93 [23], Ser422 [15], Ser425 [24], Ser498 [23] and Ser504 [23]. Ser597 phosphorylation is also known in the mouse homolog eIF4B [25]. The influence of phosphorylation on eIF4B is not well understood, but it is suggested that phosphorylation of Ser422 by S6K1 interferes with translation initiation in vivo[15]. Although we confirmed that eIF4B was phosphorylated by CaMKIId in vitro, the phosphorylation site(s) and physiological role of CaMKIId phosphorylation remain to be elucidated.

In recent years, studies of phosphorylation signaling have evolved dramatically and various approaches have been tried to elucidate phosphorylation signaling pathways. However, identification of kinase substrates has been hampered by difficulties in synthesizing sufficient quantities of functionally active recombinant proteins for biochemical analysis. Although peptide screens allow rapid characterization of the preferred primary sequence for phosphorylation by a kinase, these assays are plagued by a potential lack of specificity. In this study, we attempted to screen CaMKIId substrates from HeLa cell extracts by using crude kinase expressed in the wheat germ cell-free system. Using this system, we have successfully identified STIP1 and eIF4B as new phosphorylation target proteins. This new strategy, which can use crude kinase for screening, provides a simple and easy way to facilitate analysis of substrates for protein kinases. Because of the utilization of natural substrates, substrate specificity is more similar to the physiological reaction than when using peptides and denatured proteins. In addition, the use of crude kinases in the screening not only facilitates preparation of the kinase of interest but also may decrease the risk of deactivation of kinases suffered by screens utilizing kinases with purification tags or which have gone through purification processes. In the method described here the number of candidate substrate spots could be increased by applying, for example, fluorescent staining or silver staining which are more sensitive than CBB staining. Overlap pH isoelectric point electrophoresis and use of phospho-protein enrichment columns may also be of use in increasing the number of candidates. Although our approach has proven effective, some issues still need to be addressed and these include: (i) ensuring that the protein kinase is in the active form. (ii) Phosphorylation cannot be detected when the protein has already been phosphorylated in the cell, even if it is a physiological substrate. (iii) Proteins that have a remarkably biased p*I* such as nuclear receptor are outside the range of isoelectric focusing. (iv) Low abundance proteins are very difficult to detect.

We have therefore confirmed that phosphorylation substrates of CaMKIId can be detected using cell-free synthesized crude kinase without any purification and that the wheat cell-free system could produce functionally active kinases. These experiments indicate that our simple approach based on a wheat cell-free system is a useful tool for easy screening for substrate proteins of protein kinases in cell extracts.

Acknowledgements: We thank Keizo Oka (Department of Bioscience, INCS, Ehime University) for culture of HeLa cell lines. This work was partially supported by the Special Coordination Funds for Promoting Science and Technology by the Ministry of Education, Culture, Sports, Science and Technology, Japan (Y.E. and T.S.).

References

[1] Clapham, D.E. (1995) Calcium signaling. Cell 80, 259–268.
[2] Hudmon, A. and Schulman, H. (2002) Structure–function of the multifunctional Ca^{2+}/calmodulin-dependent protein kinase II. Biochem. J. 364, 593–611.
[3] Singh, S., Powell, D.W., Rane, M.J., Millard, T.H., Trent, J.O., Pierce, W.M., Klein, J.B., Machesky, L.M. and McLeish, K.R. (2003) Identification of the p16-Arc subunit of the Arp 2/3 complex as a substrate of MAPK-activated protein kinase 2 by proteomic analysis. J. Biol. Chem. 278, 36410–36417.
[4] Ogasawara, T., Sawasaki, T., Morishita, R., Ozawa, A., Madin, K. and Endo, Y. (1999) A new class of enzyme acting on damaged ribosomes: ribosomal RNA apurinic site specific lyase found in wheat germ. EMBO J. 18, 6522–6531.
[5] Madin, K., Sawasaki, T., Ogasawara, T. and Endo, Y. (2000) A highly efficient and robust cell-free protein synthesis system prepared from wheat embryos: plants apparently contain a suicide system directed at ribosomes. Proc. Natl. Acad. Sci. USA 97, 559–564.
[6] Sawasaki, T., Hasegawa, Y., Tsuchimochi, M., Kamura, N., Ogasawara, T., Kuroita, T. and Endo, Y. (2002) A bilayer cell-free protein synthesis system for high-throughput screening of gene products. FEBS Lett. 514, 102–105.
[7] Sawasaki, T., Ogasawara, T., Morishita, R. and Endo, Y. (2002) A cell-free protein synthesis system for high-throughput proteomics. Proc. Natl. Acad. Sci. USA 99, 14652–14657.
[8] Sawasaki, T., Hasegawa, Y., Morishita, R., Seki, M., Shinozaki, K. and Endo, Y. (2004) Genome-scale, biochemical annotation method based on the wheat germ cell-free protein synthesis system. Phytochemistry 65, 1549–1555.
[9] Endo, Y. and Sawasaki, T. (2006) Cell-free expression systems for eukaryotic protein production. Curr. Opin. Biotechnol. 17, 373–380.
[10] Sawasaki, T., Kamura, N., Matsunaga, S., Saeki, M., Tsuchimochi, M., Morishita, R. and Endo, Y. (2008) Arabidopsis HY5 protein functions as a DNA-binding tag for purification and functional immobilization of proteins on agarose/DNA microplate. FEBS Lett. 582, 221–228.
[11] Ryo, A., Togo, T., Nakai, T., Yamaguchi, A., Suzuki, K., Perrem, K., Hirayasu, Y., Liou, Y.C. and Aoki, I. (2006) The prolyl-isomerase Pin1 accumulates in the Lewy bodies of Parkinson's disease and facilitates the formation of α-synuclein inclusions. J. Biol. Chem. 281, 4117–4125.
[12] Longshaw, V.M., Chapple, J.P., Balda, M.S., Cheetham, M.E. and Blatch, G.L. (2004) Nuclear translocation of the Hsp70/Hsp90 organizing protein mSTI1 is regulated by cell cycle kinases. J. Cell. Sci. 117, 701–710.
[13] Morley, S.J. and Traugh, J.A. (1989) Phorbol esters stimulate phosphorylation of eukaryotic initiation factors 3, 4B, and 4F. J. Biol. Chem. 264, 2401–2404.
[14] Morley, S.J. and Traugh, J.A. (1990) Differential stimulation of phosphorylation of initiation factors eIF-4F, eIF-4B, eIF-3, and ribosomal protein S6 by insulin and phorbol esters. J. Biol. Chem. 265, 10611–10616.
[15] Raught, B., Peiretti, F., Gingras, A.C., Livingstone, M., Shahbazian, D., Mayeur, G.L., Polakiewicz, R.D., Sonenberg, N. and Hershey, J.W.B. (2004) Phosphorylation of eucaryotic translation initiation factor 4B Ser422 is modulated by S6 kinases. EMBO J. 23, 1761–1769.
[16] Rush, J., Moritz, A., Lee, K.A., Guo, A., Goss, V.L., Spek, E.J., Zhang, H., Zha, X.M., Polakiewicz, R.D. and Comb, M.J. (2004) Immunoaffinity profiling of tyrosine phosphorylation in cancer cells. Nat. Biotechnol. 23, 94–101.

[17] Kinoshita, E., Kinoshita-Kikuta, E., Takiyama, K. and Koike, T. (2006) Phosphate-binding tag, a new tool to visualize phosphorylated proteins. Mol. Cell. Proteomics 5, 749–757.
[18] Chen, S. and Smith, D.F. (1998) Hop as an adaptor in the heat shock protein 70 (Hsp70) and Hsp90 chaperone machinery. J. Biol. Chem. 273, 35194–35200.
[19] Odunuga, O.O., Longshaw, V.M. and Blatch, G.L. (2004) Hop: more than an Hsp70/Hsp90 adaptor protein. Bioessays 26, 1058–1068.
[20] Bharadwaj, S., Ali, A. and Ovsenek, N. (1999) Multiple components of the HSP90 chaperone complex function in regulation of heat shock factor 1 *in vivo*. Mol. Cell. Biol. 19, 8033–8041.
[21] Daniel, S., Bradley, G., Longshaw, V.M., Söti, C., Csermely, P. and Blatch, G.L. (2008) Nuclear translocation of the phosphoprotein Hop (Hsp70/Hsp90 organizing protein) occurs under heat shock, and its proposed nuclear localization signal is involved in Hsp90 binding. Biochim. Biophys. Acta 1783, 1003–1014.
[22] Gong, K.J. and Tsokos, G.C. (1996) Cell signaling and heat shock protein expression. J. Biomed. Sci. 3, 379–388.
[23] Beausoleil, S.A., Jedrychowski, M., Schwartz, D., Elias, J.E., Villen, J., Li, J., Cohn, M.A., Cantley, L.C. and Gygi, S.P. (2004) Large-scale characterization of HeLa cell nuclear phosphoproteins. Proc. Natl. Acad. Sci. USA 101, 12130–12135.
[24] Kim, J.E., Tannenbaum, S.R. and White, F.M. (2005) Global phosphoproteome of HT-29 human colon adenocarcinoma cells. J. Proteome. Res. 4, 1339–1346.
[25] Ballif, B.A., Villén, J., Beausoleil, S.A., Schwartz, D. and Gygi, S.P. (2004) Phosphoproteomic analysis of the developing mouse brain. Mol. Cell. Proteomics 3, 1093–1101.